NANO LETTERS

Letter

pubs.acs.org/NanoLett

Free-Standing Kinked Silicon Nanowires for Probing Inter- and Intracellular Force Dynamics

John F. Zimmerman,[†] Graeme F. Murray,[†] Yucai Wang,[†] John M. Jumper,[†] Jotham R. Austin, II,[‡] and Bozhi Tian*[,†,‡,§]

[†]Department of Chemistry, [‡]The Institute for Biophysical Dynamics, and [§]The James Franck Institute, University of Chicago, Chicago, Illinois 60637, United States

Supporting Information

ABSTRACT: Silicon nanowires (SiNWs) have emerged as a new class of materials with important applications in biology and medicine with current efforts having focused primarily on using substrate bound SiNW devices. However, developing devices capable of free-standing inter- and intracellular operation is an important next step in designing new synthetic cellular materials and tools for biophysical characterization. To demonstrate this, here we show that label free SiNWs can be internalized in multiple cell lines, forming robust cytoskeletal interfaces, and when kinked can serve as free-standing inter- and intracellular force probes capable of continuous extended (>1 h) force monitoring. Our results show that intercellular interactions exhibit ratcheting like behavior with force peaks of ∼69.6 pN/SiNW, while intracellular force peaks of ∼116.9 pN/SiNW were recorded during smooth muscle contraction. To accomplish this, we have introduced a simple single-capture dark-field/phase contrast optical imaging modality, scatter enhanced phase contrast (SEPC), which enables the simultaneous visualization of both cellular components and inorganic nanostructures. This approach demonstrates that rationally designed devices capable of substrate-independent operation are achievable, providing a simple and scalable method for continuous inter- and intracellular force dynamics studies.

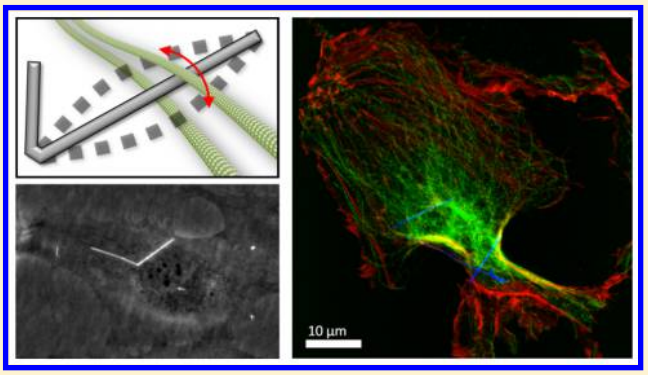

KEYWORDS: *Silicon nanowire, force dynamics, endocytosis, bionano interface, cytoskeleton*

Inorganic nanostructures are a promising class of materials for use in biology and medicine, because of their distinct length-scale and material properties. This allows them to be introduced in a minimally invasive fashion, interfacing with cellular systems on their natural length scale.[1] Recent demonstrations of nanomaterials in biology have included probes for the sensitive detection of electrical signaling,[2,3] intracellular pressures,[4] cellular fluid mechanics,[5] and specific chemical composition[6,7] with other groups using nanomaterials as drug delivery vectors,[8,9] contrast imaging reagents,[10] and as nanobionic systems.[11]

In exploring the nanomaterial/biology interface, synthetically enabled silicon nanowires (SiNWs) are of particular interest, as they can be rationally designed[12,13] and have well-defined structural and material properties,[14−16] while silicon is one of the few semiconductor materials to display low cytotoxicity.[17,18] This diverse set of material properties could potentially enable the design of a wide range of nanoscopic "building blocks" that can be applied in a biological context, leading to a host of possible device designs and applications such as intracellular electronic stimulators or biosensors. Collectively, this makes SiNWs a prime target for further investigation, however, few studies to date have experimentally examined how substrate free SiNWs (i.e., those that are not bound to macroscopic substrates) interact with cellular systems.[19,20] To demonstrate that such devices capable of substrate-independent operation are achievable, here we show that SiNWs can be internalized in a label-free manner, forming distinct junctions with cytoskeletal filaments and when kinked can serve as free-standing inter- and intracellular probes capable of continuous extended (>1 h) force monitoring.

In this study, we focused primarily on designing devices capable of monitoring the mechanical forces that cellular systems exert on their microenvironment, as these play an important role in regulating physiological processes with the extracellular matrix and cytoskeletal filaments providing mechanical cues for inter- and intracellular signaling.[21−23] Understanding these processes is an important step in designing new therapeutic tissue regeneration and drug delivery systems[24] but to date our ability to probe these systems is limited. Deformable substrate,[25−27] molecular probe,[28−30] and optical tweezer[30] methods can measure cellular force dynamics with high spatiotemporal resolution. However, there is still a need to develop a simple system capable of continuously

Received: May 19, 2015
Revised: July 9, 2015

DOI: 10.1021/acs.nanolett.5b01963
Nano Lett. XXXX, XXX, XXX−XXX

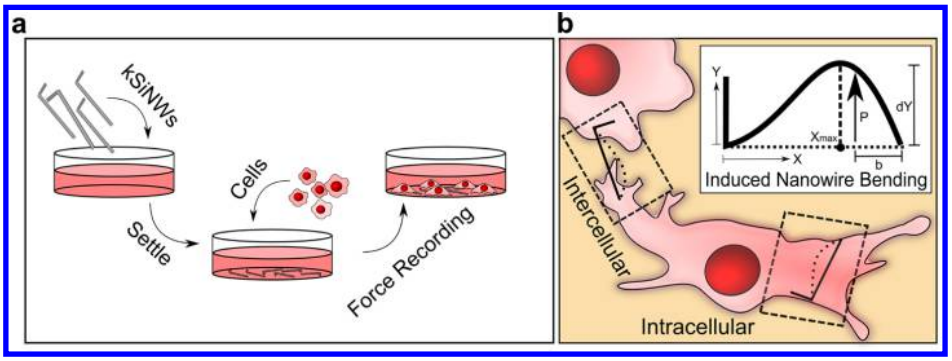

Figure 1. KSiNW-based force sensing schematics. (a) Illustration of nanowires acting as intra- and intercellular force sensors. (b) Possible interactions between KSiNW and cytoskeletal filaments with entanglement enabling force transduction dynamics. (Inset) Model of KSiNW deformation. The short arm (vertical beam, left) anchors the KSiNW, while the longer arm experiences cellular induced bending. *P*, *b*, and *dY* are the load, its distance from the tip, and the deflection respectively, while x_{max} is the *x*-position of the maximum deflection.

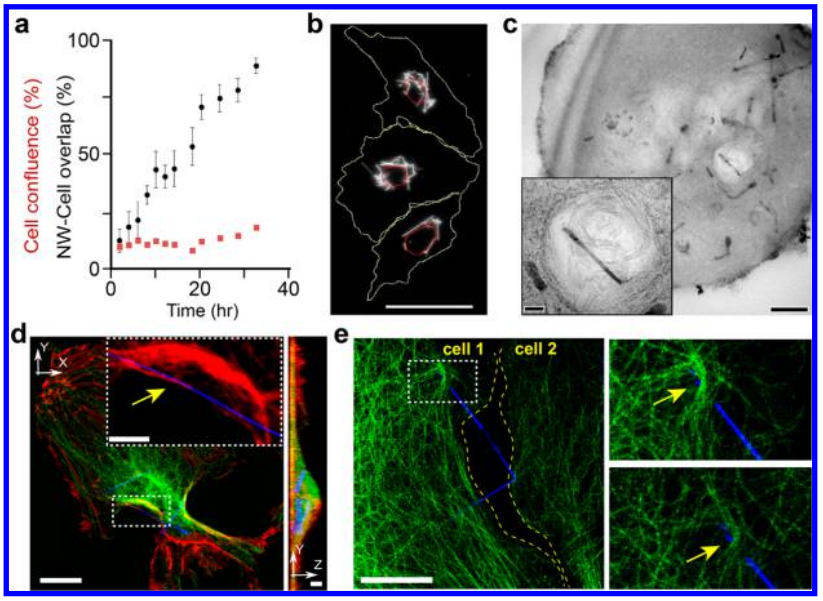

Figure 2. Internalization of SiNWs and their intra- and intercellular interfaces. (a) Ensemble rate of NW-cell overlap (black line) as compared to cell confluence (red line) indicating preferential NW-cell interactions. (b) Dark-field image of colocalized SiNWs, overlaid with the cell's membrane (yellow) and nucleus (red). Scale bar, 50 μm. (c) TEM micrograph of a thin section of HUVEC (thickness, ~200 nm) demonstrating internalized SiNWs. Scale bar, 2 μm. Higher-magnification inset of a SiNW contained in a vacuole. Scale bar, 400 nm. (d) Confocal fluorescence (HUVEC, red-actin, green-tubulin) micrograph in $x-y$ (left) and $y-z$ (right) planes, containing NWs (blue-scattering). Actin channel inset shows entangled SiNWs. Scale bars, 10 μm (left), 2.5 μm (left, inset), and 2 μm (right). (e) Time-lapse live cell confocal fluorescence micrograph, showing HASMC microtubule bundles (green) interacting with a KSiNW (blue) at T = 0 min (left, and upper right) and T = 24 min (lower right). Scale bars, 10 μm (left) and 5 μm (right).

probing inter- and intracellular forces over long time scales. Optimally, this system would be resistant to both localized photothermal heating[31,32] and fluorescent bleaching,[33] as these limit experimental time-scales.

With this in mind, kinked silicon nanowires (KSiNWs) were selected as potential cellular force probes. First, as KSiNWs are easily distributed in a druglike fashion to cellular systems (Figure 1a), they are relatively simple to implement and can be used in wide array of experimental conditions to monitor both inter- and intracellular force processes (Figure 1b). Second, the kinked structure serves as both a visual (Supporting Information Figure S1a) and physical anchor, limiting device rotation and translation, ensuring that force is transduced primarily to mechanical strain. The operational principle of this platform, relies on the maintained force-strain relationship between nanowires and their microenvironment (Figure 1). Nanowire crystal deformation results in the buildup of stress and the generation of an elastic restorative force. To prevent relaxation a consistent force must be applied to the wire. Therefore, by monitoring the structural deformations of the SiNW, the present force being applied to the wire can be determined. As a result, KSiNWs can be used as a platform to study the spatial-temporal evolution of forces that cellular systems exert on their microenvironment.

In order to retrieve this structural deformation information and enable the use of these devices, we have introduced a new optical technique, scatter enhanced phase contrast (SEPC) microscopy, a simple to implement dark-field/phase contrast optical imaging modality, which allows the long-term monitoring of KSiNW/cellular interactions. This method requires only low intensity light sources, and is therefore easily implemented using most conventional microscopy setups, requiring only slight modification (i.e., the installation of an inexpensive, commercially available ring LED emitter). Addi-

DOI: 10.1021/acs.nanolett.5b01963
Nano Lett. XXXX, XXX, XXX−XXX

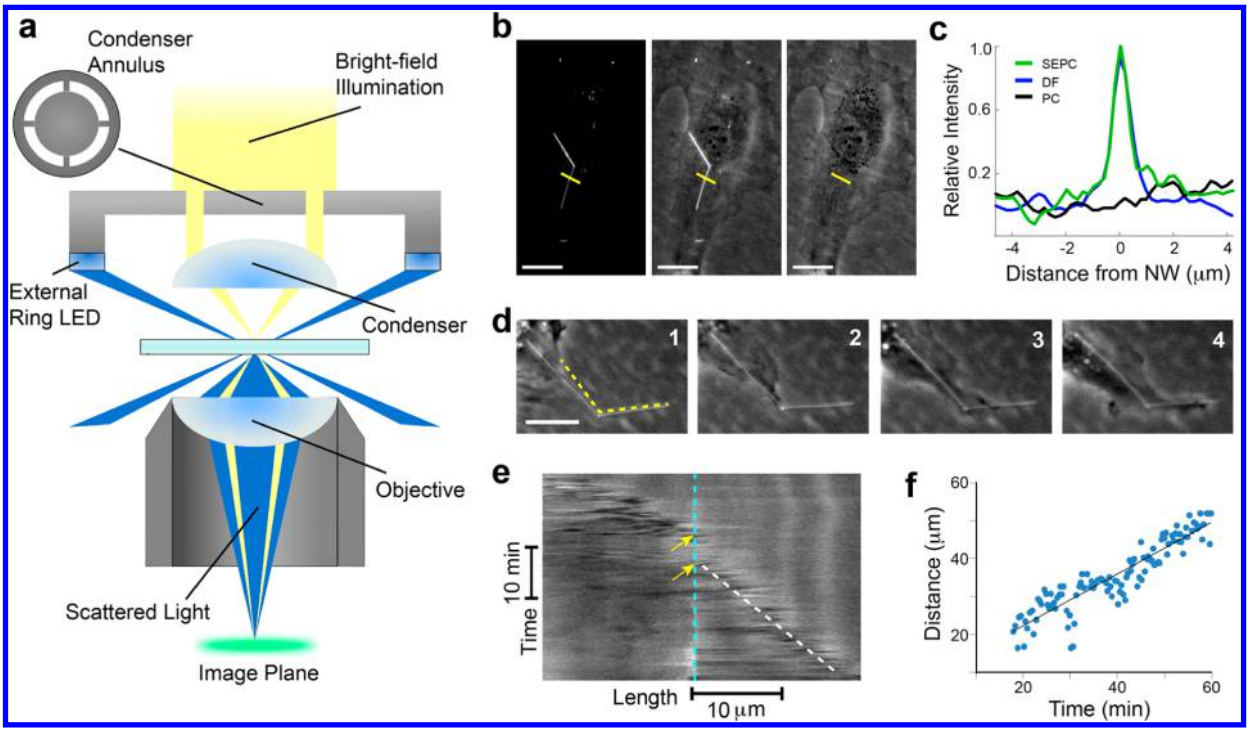

Figure 3. SEPC imaging modality. (a) SEPC light path diagram. (b,c) Images (b) and line plots taken over the same region in b (yellow line) (c), indicating the relative signal intensity of NWs under: dark-field (b, left; c, blue), SEPC (b, middle; c, green), and phase contrast (b, right; c, black). Scale bars in b, 10 μm. (d,e) Time-lapse SEPC micrograph of a membrane extending along a KSiNW (HUVEC, 10 min elapsed/frame) with associated kymograph (e) (dashed cyan line, kink location) taken from the indicated path (dashed yellow in d). Scale bar, 10 μm. (f) Membrane extension along the KSiNW extracted from the kymograph. The slope of the linear fit yields the rate of 11.34 ± 0.05 nm/s (R^2 = 0.84).

tionally, the use of low intensity light sources and the avoidance of fluorescent tags, mark this method as being resistant to both photobleaching and photothermal effects,[34] making it appropriate for long-term continuous force studies. Here we demonstrate studies of >1 h, while in principle this period could be substantially expanded. Given the relative ease of implementation and extended time-scales of these studies, this technique offers substantial promise for researchers interested in exploring nanobiointeractions where both inorganic and biological components can be imaged simultaneously. Additionally, this approach in general demonstrates that devices capable of substrate-independent operation are achievable and can be internalized in human cell lines.

To confirm that label-free SiNWs interact with single cells, human umbilical vascular endothelial cells (HUVECs) and human aortic smooth muscle cells (HASMCs) were selected as model cell lines, as endothelial cells constitute the interior layer of blood vessels where future in vivo applications can target, while smooth muscle cells enable muscle contraction studies. Ensemble dynamics were studied, measuring the relative NW-cell overlap as a function of incubation time (Supporting Information Figure S2) with HUVECs (Figure 2a) and HASMCs (Supporting Information Figure S3a) showing ~86% and ~56% NW colocalization, respectively, after 24 h. While colocalization does not report directly on internalization, it indicates a preferential interaction, as a noncoupled system would be expected to show no better colocalization than random (i.e., no better than cell confluence; depicted in red). Additionally, SiNWs were observed to cluster in the perinuclear region (Figure 2b) but were excluded from the nuclear envelope, further suggesting SiNWs internalization.

To confirm that SiNWs were being endocytosed, two separate methods were used. First, trypsinized cells were rapidly cryo-fixed and processed using high pressure freezing and freeze substitution techniques.[35] Thin cell sections (~200 nm) were imaged using transmission electron microscopy (TEM) with the resulting micrographs containing SiNW fragments in both the cytosol and vacuoles (Figure 2c, Supporting Information Figure S4). Internalization was further confirmed using confocal microscopy with fluorescently labeled actin (red) and tubulin (green), while SiNWs were visualized using scattered light (blue). Whole cell volumes were three-dimensionally (3D) reconstructed with NWs present in both HUVECs (Figure 2d) and HASMCs (Supporting Information Figure S3b).

During this process, KSiNWs were found to be entangled in the cytoskeleton network, forming junctions with both actin (Figure 2d, inset) and microtubules (Figure 2e), causing the KSiNWs to become pinned intra- (Figure 2d) and intercellularly (Figure 2e). Using live cell staining, we tracked microtubule/KSiNW junctions (Figure 2e, right), some of which were maintained over an extended period (≥24 min). This entanglement with the cytoskeleton represents a distinct SiNW-protein interaction, the first of its kind reported, and suggests a mechanism of KSiNW anchoring and intra/intercellular force transduction, where cytoskeleton and cytosolic rearrangements processes can result in the bending of filamentous KSiNWs. Studying these KSiNW deformations, we were able to infer the overall cellular force dynamics, enabling the use of these nanoscale devices as intracellular force probes.

While confocal techniques display clear NW and cellular features, they are prone to photobleaching and other

DOI: 10.1021/acs.nanolett.5b01963
Nano Lett. XXXX, XXX, XXX−XXX

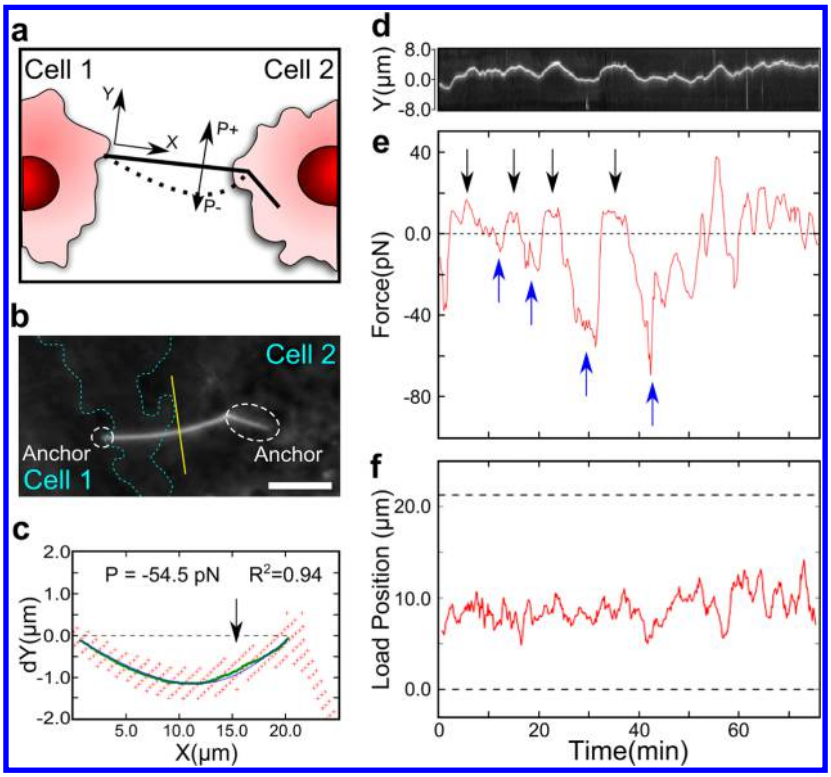

Figure 4. Intercellular force sensing. (a) Illustration of HUVEC KSiNW intercellular interactions with associated SEPC micrograph (scale bar 5 μm) (b), showing a bent SiNW state (dashed cyan lines, cell membranes). (c) Example single-frame force fitting data for the displayed NW bending (T = 31 min) (red, raw coordinates; green, curve average; blue, fit to the curve average; arrow, estimated load position). (d) Kymograph (from yellow line segment in b) and time-lapse (e) force data with coincident load position (f), showing ratcheting force behavior (shared time axis) (arrows indicating ratcheting force peaks).

undesirable consequences of laser/Si interactions such as the local SiNW-induced photothermal heating of cells.[34] To enable the extended noninvasive study of nanobiointeractions, we introduced a simple optical microscopy technique, scatter enhanced phase contrast (SEPC), which uses the one-shot acquisition of both dark-field (DF) and phase contrast (PC) images (Figure 3, Supporting Information Figure S5). SiNWs are radially below the optical resolution limit reducing their visibility using bright field methods (e.g., PC). However, they also possess a high refractive index, appearing readily under DF. Adherent cells on the other hand have a low refractive index and are obscured using DF. To bridge this gap an oblique angle ring emitter was employed (Figure 3a), using simultaneously transmitted DF and PC projections to create a single SEPC image. This allowed for the clear visualization of both SiNWs and cellular features (Figure 3b), yielding an average 3.6-fold improvement in signal-to-noise ratio (S/N) of NWs in HUVECs as compared to PC (Figure 3c). The ability of SEPC to dynamically track both cells and nanomaterials in a label-free manner allows SiNW interactions to be linked to specific cellular processes. One example is the recording of HUVEC membrane extension along a single KSiNW (Figure 3d, Supporting Information Video S1). Using SEPC, a kymograph was obtained of the cell membrane (Figure 3e). By mapping the leading edge position, a linear relationship was established showing that the wire is engulfed at an average rate of 11.34 ± 0.05 nm/s (Figure 3e, white dashed line, and Figure 3f), after pausing at the kinked joint for ∼9 min (Figure 3e, yellow arrows). The observation that the leading edge of the cell membrane tightly followed the orientation of the KSiNW highlights the ability of the cell to recognize nanoscale topographies and suggests that SiNWs can yield enhanced cell/substrate interactions. Additionally, we note here that SEPC is not strictly limited to SiNW identification but can be readily adapted to work in conjunction with other nanomaterials. As a result, this technique has strong implications for other forms of biological nanoparticle tracking, such as carbon nanotubes and gold nanoparticle internalization studies.

Using SEPC microscopy, time-lapse force dynamics were extracted from KSiNW conformations with the NWs coordinates (x,y) determined using a custom built-script in NIH's ImageJ (Supporting Information Figure S6, S7). KSiNWs were modeled as simply supported beams with an asymmetric load, using Euler–Bernoulli beam theory. This model provided a good match between predicted and experimentally observed deflections, is generalizable to a wide range of load conditions, is computationally quick, and yields information on the position of the force load, with the deformation of the wire being given by

$$dY(x) = \begin{cases} \dfrac{Pbx(L^2 - b^2 - x^2)}{6LEI} & 0 \le x \le L - b \\ \dfrac{Pbx(L^2 - b^2 - x^2)}{6LEI} + \dfrac{P(x - L + b)^3}{6EI} & L - b < x \le L \end{cases} \quad (1)$$

where P is the force of the load (Figure 1c), L is the length of the wire, b is the position of the point-load (Figure 1b), E and I are the elastic Young's modulus and the beams' cross sectional moment of inertia, respectively ($I = (5\sqrt{3})/(144)D^4$, where D is the NW diameter). KSiNWs were grown primarily in the ⟨112⟩ direction and a Young's modulus of 169 GPa[14,36] was used with the location of the point load, b, determined on a frame-by-frame basis using the geometric relationship

DOI: 10.1021/acs.nanolett.5b01963
Nano Lett. XXXX, XXX, XXX−XXX

$$b = \sqrt{L^2 - 3x_{max}^2} \quad (2)$$

where x_{max} is the x-coordinate of maximum deflection (Figure 1b) whose value was obtained using a 10-point moving average.[37] Force was determined using a least-squares regression of eq 2, fitting for the load parameter, P. KSiNW force probes with an average diameter of ∼28.1 nm (as measured by TEM) were selected, as they afforded a wide detection range with a maximum observed force of ∼5400 pN and a minimum detection limit of ∼1.8 pN. However, in principle this range can be controllably tuned to specific biological processes by adjusting the nanowire width, a processes that can be readily achieved synthetically. By tuning the NW diameter's, the NW's moment of inertia and size dependent modulus of elasticity[14,15] are effected, which are directly related to the observed force via eq 2.

In using this mechanical model there are a few considerations. First, in a real system the exact load configuration is a three-dimensional composite of both cytoskeleton and cytosolic forces, however here we have assumed a two-dimensional point-like load. This is a fine approximation as it provides a good estimate for the total sum of the component forces experienced by the SiNW in the x,y dimension, however additional out of plane forces may be also be experienced. Second, this model assumes spatially pinned edges, an assumption that is reasonable given the NWs are ∼30 μm long with the tips showing an average velocity of less than 1.4 μm/min (<5% displacement/min) (Supporting Information Videos S2 and S3), which is on par with the underlying cell's motility. Additionally, we have found that the deformations predicted using these boundary conditions matched well with experimentally observed values (Supporting Information Figure S7). Finally, while the current model is robust to a wide range of load conditions, we note that other force models could be considered for future use, such as local curvature[37,38] and finite element[39] analysis methods.

Using this model, we examined the intercellular forces exerted on a KSiNW by two HUVECs competing to internalize the same NW and the intracellular forces exerted by HASMC during drug-induced constriction. For HUVECs, a KSiNW was captured midway through the internalization process (Figures 4a,b) with both ends pinned, one on the membrane of an adjacent cell and the other connected to the internalizing cell (Figure 4b). Force was recorded perpendicular to the axis of the extended KSiNW arm with HUVECs exhibiting unexpected ratcheting like behavior (Figure 4c–f), jostling the NW back and forth by applying forces with increasing either amplitude or duration (Figure 4e, highlighted with arrows). The load force fitting (Figure 4c) and load position predictions for one typical frame are given (marked with the arrow, Figure 4c), suggesting that the present model yields reasonable results and predictions (see more details in Supporting Information Figure S7, Video S2). Force dynamics (Figure 4e) were smoothed using a five-frame moving average, resulting in a force profile similar to the corresponding kymograph (Figure 4d). Under these conditions, the KSiNW was observed to experience a maximum averaged force peak of 69.6 pN (Figure 4e). The load position dynamics (Figure 4f) suggests that the lamellipodium was the primary location where NW bending occurred, a reasonable outcome given focal adhesions exhibit high density at lamellipodium.[23] Additionally, the NW length (i.e., the distance between the left tip and the middle kink) variation was only ∼2.5% (±SD, Supporting Information Figure S8), suggesting that possible force contributions due to NW buckling and torque are minor. As silicon materials can dissolve under physiological conditions,[40] probe integrity was ensured using the scattering intensity of KSiNWs submerged in media with no significant change noted over 72 h (Supporting Information Figure S9). The observed ratcheting behavior is likely exhibited by the cell (cell 2) in an attempt to free the KSiNW from the underlying substrate and the "competing" cell (cell 1).

Finally, we studied intracellular force dynamics using fully internalized KSiNWs in HASMCs (Figure 5, Supporting Information Video S3). Vasoconstriction was examined, inducing contraction using the hormone angiotensin II (ANGII). A KSiNW located in the lamella was observed (Figure 5b) with force data recorded intracellularly at an angle of 52.6° (Figure 5a). Upon the introduction of ANGII (t = 0 min), a relaxation of tension was observed (Figure 5c), presumably due to cytoskeleton rearrangement, reaching a minimum force of 11.0 pN (Figure 5c, arrow 1), which was followed by a significant force peak (t = ∼30 min, between dashed green lines, Figure 5c) with a maximum force of 116.9 pN (Figure 5c, arrow 2) and a minimally strained state (Figure 5c, arrow 3). Different from the extracellular case (Figure 4d), the predicted load position dynamics (Figure 5d) suggests significant spatial evolution of intracellular forces over a single cytoskeleton-like KSiNW, especially during the peaked force actuation period (between dashed green lines, Figure 5d). An example frame of the force fitting data is provided (Supporting Information Figure S10). Unexpectedly, no obvious morphology change was noted in the lamella containing the KSiNW (the region between yellow dashed lines, Figure 5b) during the observed force cycle. This highlights the usefulness of intracellular force measurements in improving biophysical characterization, as purely external force measurements may

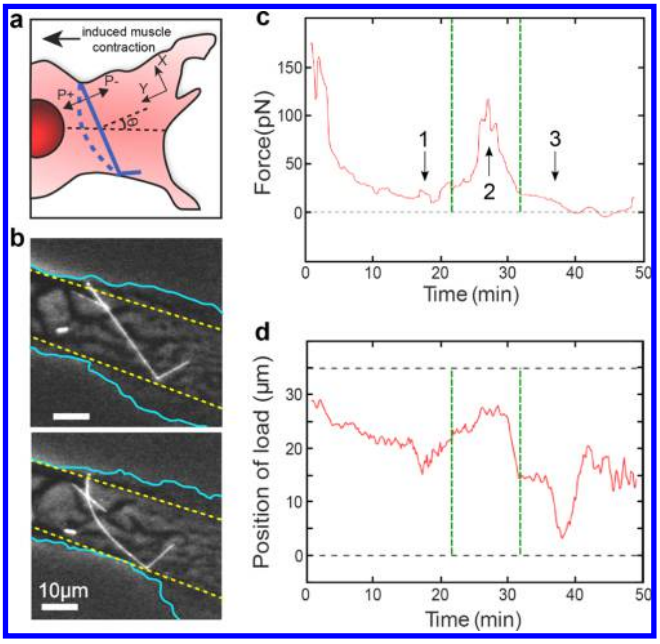

Figure 5. Intracellular force sensing. (a) Schematic of HASMC contraction. (b) Associated SEPC micrographs, showing straight (upper)/bent (lower) states (cyan, cell membranes; yellow, lamella boundary). (c,d) Time-lapse force data (c) with coincident load position (d), showing well-defined contraction peak (between dashed green lines).

DOI: 10.1021/acs.nanolett.5b01963
Nano Lett. XXXX, XXX, XXX−XXX

show this portion of the cell as being nonresponsive to hormone treatment during this period.

This work demonstrates that rationally designed devices capable of independent inter- and intracellular operation are achievable with SiNWs serving as a potential platform technology for designing future constructs. In our studies we have shown long-term noninvasive probes for force monitoring that were used for several hours without marked deleterious effects, however in principle this range could be substantially extended as KSiNWs are not subject to photobleaching and the use of conventional light sources produces only negligible localized photothermal heating.[31] In comparing this method to other intracellular force measurement technique methods such as optical trapping, there are some limitations, including target specificity. However, this technique offers several possible advantages. First, this technique is easily implemented, with the nanoscale force probes being administrated in a similar fashion to drugs. This raises the possibility of using additional force probes within a single experiment, incorporating multiple devices both within an individual cell and across a cellular network. This multiplexed signal detection could be used to studying ensemble force transduction dynamics and is not easily achieved in other intracellular force detection methods. Second, the tunable nature of these probes makes them adjustable to a wide array of force conditions with the detection range depending on the material properties of the probe and not the optical setup. This makes adjusting these probes relatively noninvasive compared to optical traps whose detection limits are dependent on laser strength,[41] which can lead to significant localized heating.[31,32,41]

This work also raises several intriguing possibilities from a biomaterials perspective, enabling studies into how nanomaterials can affect intracellular force interactions and mechanosignaling. First, we believe that SEPC is a generalizable method that can be used in conjunction with other nanoscale devices to help elucidate how nanomaterials interact in a dynamic manner with cellular systems. As researchers begin to push into this field, we feel that SEPC will serve as a platform for expanded device characterization. Second, the measurements presented here suggest that similar mechanical processes may occur in individual biological filaments and highlight the mechanical considerations needed for designing future nanoscale probes and therapeutic devices. For instance, one could imagine designing a nanoscale piezoelectric device,[42] capable of independent intracellular operation, with this work serving as a basis for understanding the limits of such a system. Finally, as SiNWs are observable even through tissue samples,[43] we hope that this work can be used in future in vivo experiments, where intracellular forces are particularly difficult to probe.

■ ASSOCIATED CONTENT

Supporting Information

A detailed explanation of the device synthesis, materials, and methods, including a more in-depth look at SEPC techniques is given. Additional supplementary figures and supplementary videos are included. The Supporting Information is available free of charge on the ACS Publications website at DOI: 10.1021/acs.nanolett.5b01963.

■ AUTHOR INFORMATION

Corresponding Author

*E-mail: btian@uchicago.edu.

Author Contributions

B.T. supervised the research. J.F.Z., G.F.M., Y.W., and J.R.A. performed the experiments. J.F.Z., G.F.M., J.M.J., and B. T. analyzed the data. J.F.Z. and B.T. wrote the manuscript with input from other coauthors.

Notes

The authors declare no competing financial interest.

■ ACKNOWLEDGMENTS

This work is supported by Air Force Office of Scientific Research (AFOSR FA9550-14-1-0175), National Science Foundation (NSF CAREER, DMR-1254637; NSF MRSEC, DMR-0820054), Searle Scholars Foundation, and the University of Chicago start-up fund.

■ ABBREVIATIONS

SiNWs, silicon nanowires; KSiNWs, kinked silicon nanowires; SEPC, scatter enhanced phase contrast; PC, phase contrast; DF, dark field; HASMC(s), human aortic smooth muscle cells; HUVEC(s), human umbilical vascular endothelial cells; LED, light-emitting diode; TEM, transmission electron microscopy; Ang II, angiotensin II

■ REFERENCES

(1) Whitesides, G. The'right'size in Nanobiotechnology. *Nat. Biotechnol.* **2003**, *21*, 1161−1165.
(2) Zimmerman, J.; Parameswaran, R.; Tian, B. Nanoscale Semiconductor Devices as New Biomaterials. *Biomater. Sci.* **2014**, *2*, 619.
(3) Tian, B.; Cohen-Karni, T.; Qing, Q.; Duan, X.; Xie, P.; Lieber, C. M. Three-Dimensional, Flexible Nanoscale Field-Effect Transistors as Localized Bioprobes. *Science* **2010**, *329*, 830−834.
(4) Gómez-Martínez, R.; Hernández-Pinto, A. M.; Duch, M.; Vázquez, P.; Zinoviev, K.; de la Rosa, E. J.; Esteve, J.; Suárez, T.; Plaza, J. a. Silicon Chips Detect Intracellular Pressure Changes in Living Cells. *Nat. Nanotechnol.* **2013**, *8*, 517−521.
(5) Keren, K.; Yam, P. T.; Kinkhabwala, A.; Mogilner, A.; Theriot, J. a. Intracellular Fluid Flow in Rapidly Moving Cells. *Nat. Cell Biol.* **2009**, *11*, 1219−1224.
(6) Yan, R.; Park, J.-H.; Choi, Y.; Heo, C.-J.; Yang, S.-M.; Lee, L. P.; Yang, P. Nanowire-Based Single-Cell Endoscopy. *Nat. Nanotechnol.* **2011**, *7*, 191−196.
(7) Zimmerman, J.; Tian, B. Nanowire Biosensors. In *Semiconductor Nanowires: From Next-Generation Electronics to Sustainable Energy*; The Royal Society of Chemistry: Cambridge, 2015; Chapter 4, pp 167−199.
(8) Korin, N.; Kanapathipillai, M.; et al. Shear-Activated Nanotherapeutics for Drug Targeting to Obstructed Blood Vessels. *Science (Washington, DC, U. S.)* **2012**, *337*, 738−742.
(9) Kwon, N. H.; Beaux, M. F.; Ebert, C.; Wang, L.; Lassiter, B. E.; Park, Y. H.; McIlroy, D. N.; Hovde, C. J.; Bohach, G. a. Nanowire-Based Delivery of Escherichia Coli O157 Shiga Toxin 1 A Subunit into Human and Bovine Cells. *Nano Lett.* **2007**, *7*, 2718−2723.
(10) Cieplak, M. Quantum Dots as Probes in Biology. *J. Phys.: Condens. Matter* **2013**, *25*, 190301.
(11) Giraldo, J. P.; Landry, M. P.; Faltermeier, S. M.; McNicholas, T. P.; Iverson, N. M.; Boghossian, A. A.; Reuel, N. F.; Hilmer, A. J.; Sen, F.; Brew, J. A.; et al. Plant Nanobionics Approach to Augment Photosynthesis and Biochemical Sensing. *Nat. Mater.* **2014**, *13*, 1−9.
(12) Tian, B.; Xie, P.; Kempa, T. J.; Bell, D. C.; Lieber, C. M. Single-Crystalline Kinked Semiconductor Nanowire Superstructures. *Nat. Nanotechnol.* **2009**, *4*, 824−829.
(13) Tian, B.; Zheng, X.; Kempa, T. J.; Fang, Y.; Yu, N.; Yu, G.; Huang, J.; Lieber, C. M. Coaxial Silicon Nanowires as Solar Cells and Nanoelectronic Power Sources. *Nature* **2007**, *449*, 885−889.

DOI: 10.1021/acs.nanolett.5b01963
Nano Lett. XXXX, XXX, XXX−XXX

(14) Zhu, Y.; Xu, F.; Qin, Q.; Fung, W. Y.; Lu, W. Mechanical Properties of Vapor-Liquid-Solid Synthesized Silicon Nanowires. *Nano Lett.* **2009**, *9*, 3934−3939.
(15) Hsin, C.-L.; Mai, W.; Gu, Y.; Gao, Y.; Huang, C.-T.; Liu, Y.; Chen, L.-J.; Wang, Z.-L. Elastic Properties and Buckling of Silicon Nanowires. *Adv. Mater.* **2008**, *20*, 3919−3923.
(16) Ryu, S. Y.; Xiao, J.; Park, W. Il; Son, K. S.; Huang, Y. Y.; Paik, U.; Rogers, J. a. Lateral Buckling Mechanics in Silicon Nanowires on Elastomeric Substrates. *Nano Lett.* **2009**, *9*, 3214−3219.
(17) Fine, D.; Grattoni, A.; Goodall, R.; Bansal, S. S.; Chiappini, C.; Hosali, S.; van de Ven, A. L.; Srinivasan, S.; Liu, X.; Godin, B.; et al. Silicon Micro- and Nanofabrication for Medicine. *Adv. Healthcare Mater.* **2013**, *2*, 632−666.
(18) Marcon, L.; Boukherroub, R. Biocompatibility of Semiconducting Silicon Nanowires. In *Semiconducting Silicon Nanowires for Biomedical Applications*; Coffer, J. L., Ed.; Woodhead Publishing: Cambridge, 2014; pp 62−85.
(19) Zhang, W.; Tong, L.; Yang, C. Cellular Binding and Internalization of Functionalized Silicon Nanowires. *Nano Lett.* **2012**, *12*, 1002−1006.
(20) Wierzbicki, R.; Købler, C.; Jensen, M. R. B.; Lopacińska, J.; Schmidt, M. S.; Skolimowski, M.; Abeille, F.; Qvortrup, K.; Mølhave, K. Mapping the Complex Morphology of Cell Interactions with Nanowire Substrates Using FIB-SEM. *PLoS One* **2013**, *8*, e53307.
(21) Wang, N.; Butler, J. P.; Ingber, D. E. Mechanotransduction across the Cell Surface and through the Cytoskeleton. *Science* **1993**, *260*, 1124−1127.
(22) Fletcher, D. a; Mullins, R. D. Cell Mechanics and the Cytoskeleton. *Nature* **2010**, *463*, 485−492.
(23) Geiger, B.; Spatz, J. P.; Bershadsky, A. D. Environmental Sensing through Focal Adhesions. *Nat. Rev. Mol. Cell Biol.* **2009**, *10*, 21−33.
(24) Rehfeldt, F.; Engler, A. J.; Eckhardt, A.; Ahmed, F.; Discher, D. E. Cell Responses to the Mechanochemical Microenvironment−Implications for Regenerative Medicine and Drug Delivery. *Adv. Drug Delivery Rev.* **2007**, *59*, 1329−1339.
(25) Legant, W. R.; Miller, J. S.; Blakely, B. L.; Cohen, D. M.; Genin, G. M.; Chen, C. S. Measurement of Mechanical Tractions Exerted by Cells in Three-Dimensional Matrices. *Nat. Methods* **2010**, *7*, 969−971.
(26) Fischer, R. S.; Myers, K. A.; Gardel, M. L.; Waterman, C. M. Stiffness-Controlled Three-Dimensional Extracellular Matrices for High-Resolution Imaging of Cell Behavior. *Nat. Protoc.* **2012**, *7*, 2056−2066.
(27) Li, Z.; Song, J.; Mantini, G.; Lu, M. Y.; Fang, H.; Falconi, C.; Chen, L. J.; Wang, Z. L. Quantifying the Traction Force of a Single Cell by Aligned Silicon Nanowire Array. *Nano Lett.* **2009**, *9*, 3575−3580.
(28) Grashoff, C.; Hoffman, B. D.; Brenner, M. D.; Zhou, R.; Parsons, M.; Yang, M. T.; McLean, M. a; Sligar, S. G.; Chen, C. S.; Ha, T.; et al. Measuring Mechanical Tension across Vinculin Reveals Regulation of Focal Adhesion Dynamics. *Nature* **2010**, *466*, 263−266.
(29) Wang, X.; Ha, T. Defining Single Molecular Forces Required to Activate Integrin and Notch Signaling. *Science* **2013**, *340*, 991−994.
(30) Oddershede, L. B. Force Probing of Individual Molecules inside the Living Cell Is Now a Reality. *Nat. Chem. Biol.* **2012**, *8*, 879−886.
(31) Peterman, E. J. G.; Gittes, F.; Schmidt, C. F. Laser-Induced Heating in Optical Traps. *Biophys. J.* **2003**, *84*, 1308−1316.
(32) Neuman, K. C.; Chadd, E. H.; Liou, G. F.; Bergman, K.; Block, S. M. Characterization of Photodamage to Escherichia Coli in Optical Traps. *Biophys. J.* **1999**, *77*, 2856−2863.
(33) Marawske, S.; Dörr, D.; Schmitz, D.; Koslowski, A.; Lu, Y.; Ritter, H.; Thiel, W.; Seidel, C. a M.; Kühnemuth, R. Fluorophores as Optical Sensors for Local Forces. *ChemPhysChem* **2009**, *10*, 2041−2048.
(34) Roder, P. B.; Pauzauskie, P. J.; Davis, E. J. Nanowire Heating by Optical Electromagnetic Irradiation. *Langmuir* **2012**, *28*, 16177−16185.
(35) Austin, J. R., II High-Pressure Freezing and Freeze Substitution of Arabidopsis for Electron Microscopy. In *Arabidopsis Protocols*; Sanchez-Serrano, J. J., Salinas, J., Eds.; Methods in Molecular Biology; Humana Press: Totowa, NJ, 2014; Vol. *1062*, pp 473−486.
(36) San Paulo, a.; Bokor, J.; Howe, R. T.; He, R.; Yang, P.; Gao, D.; Carraro, C.; Maboudian, R. Mechanical Elasticity of Single and Double Clamped Silicon Nanobeams Fabricated by the Vapor-Liquid-Solid Method. *Appl. Phys. Lett.* **2005**, *87*, 053111.
(37) Qin, Q.; Zhu, Y. Static Friction between Silicon Nanowires and Elastomeric Substrates. *ACS Nano* **2011**, *5*, 7404−7410.
(38) Strus, M. C.; Lahiji, R. R.; Ares, P.; López, V.; Raman, A.; Reifenberger, R. Strain Energy and Lateral Friction Force Distributions of Carbon Nanotubes Manipulated into Shapes by Atomic Force Microscopy. *Nanotechnology* **2009**, *20*, 385709.
(39) Yvonnet, J.; Mitrushchenkov, a.; Chambaud, G.; He, Q. C. Finite Element Model of Ionic Nanowires with Size-Dependent Mechanical Properties Determined by Ab Initio Calculations. *Comput. Methods Appl. Mech. Eng.* **2011**, *200*, 614−625.
(40) Kang, S.-K.; Park, G.; Kim, K.; Hwang, S.-W.; Cheng, H.; Shin, J.; Chung, S.; Kim, M.; Yin, L.; Lee, J. C.; et al. Dissolution Chemistry and Biocompatibility of Silicon- and Germanium-Based Semiconductors for Transient Electronics. *ACS Appl. Mater. Interfaces* **2015**, *7*, 9297−9305.
(41) Kuo, S. C. Using Optics to Measure Biological Forces and Mechanics. *Traffic* **2001**, *2*, 757−763.
(42) Wang, Z. L.; Song, J. Piezoelectric Nanogenerators Based on Zinc Oxide Nanowire Arrays. *Science* **2006**, *312*, 242−246.
(43) Jung, Y.; Tong, L.; Tanaudommongkon, A.; Cheng, J.-X.; Yang, C. In Vivo and in Vivo Nonlinear Optical Imaging of Silicon Nanowires. *Nano Lett.* **2009**, *9*, 2440−2444.

DOI: 10.1021/acs.nanolett.5b01963
Nano Lett. XXXX, XXX, XXX−XXX